Dyes and Pigments 80 (2009) 233–238

Contents lists available at ScienceDirect

Dyes and Pigments

journal homepage: www.elsevier.com/locate/dyepig

The use of indoline dyes in a zinc oxide dye-sensitized solar cell

Masaki Matsui [a,*], Akira Ito [a], Masaya Kotani [a], Yasuhiro Kubota [a], Kazumasa Funabiki [a], Jiye Jin [b], Tsukasa Yoshida [c], Hideki Minoura [c], Hidetoshi Miura [d]

[a] Department of Materials Science and Technology, Faculty of Engineering, Gifu University, Yanagido, Gifu 501-1193, Japan
[b] Department of Chemistry, Faculty of Science, Shinshu University, 3-1-1 Asahi, Matsumoto, Nagano 390-8621, Japan
[c] Environmental and Renewable Energy System Division, Graduate School of Engineering, Gifu University, Yanagido, Gifu 501-1193, Japan
[d] Chemicrea Co. Ltd., 2-1-6 Sengen, Tsukuba, Ibaragi 305-0047, Japan

ARTICLE INFO

Article history:
Received 20 May 2008
Received in revised form 7 July 2008
Accepted 9 July 2008
Available online 25 July 2008

Keywords:
Indoline dyes
Dye-sensitized solar cell
Zinc oxide: sensitizers

ABSTRACT

The effects of the position and the type of carboxyl anchor group in double rhodanine-type indoline dyes on the performance of a zinc oxide dye-sensitized solar cell were examined. The optimum position for the carboxymethyl group was on the inner rhodanine moiety; a carboxymethyl group gave optimum results among carboxymethyl, -ethyl, and -propyl derivatives.

1. Introduction

Much attention has been paid to survey of sensitizers for dye-sensitized solar cell. Several organic dyes such as styryls [1–3], coumarins [4–7], polyenes [8–13], dimethylfluorenyl-containing dyes [14,15], and indoline dyes [16–19] have been proposed as the sensitizers. The double rhodanine indoline dye named D149 has been reported to show the highest solar-to-electricity conversion efficiency (η) among them [16]. Therefore, it is of significance to examine the effect of substituents in the double rhodanine indoline dyes on the cell performance. Meanwhile, the convenient preparation of porous zinc oxide film at low temperature has been reported [20]. This film is used as a semiconductor for dye-sensitized solar cell [21–24]. We report herein the effect of position and kind of carboxyl anchor group in double rhodanine indoline dyes on the performance of zinc oxide dye-sensitized solar cell.

2. Results and discussion

2.1. Synthesis

Indoline dyes **24**–**30** were synthesized as shown in Scheme 1. Compound **1** was allowed to react with aromatic bromides **2**–**6** to give *N*-aryl derivatives **7**–**11**, followed by formylation to afford **12**–**16**. In the cases of ethoxycarbony derivatives **13**–**15**, the ester moiety was hydrolyzed to give the corresponding carboxylic acids **17**–**19**. Finally, aldehydes **12** and **16**–**19** were allowed to react with active methylene-containing double rhodanines **20**–**23** in the presence of base to give **24**–**30**.

2.2. UV–vis absorption and fluorescence spectra

The UV–vis absorption and fluorescence spectra of **24**–**27** and **28**–**30** are shown in Figs. 1 and 2, respectively. The results are also listed in Table 1. The indoline dyes **24**–**27** showed absorption maxima (λ_{max}) in the range of 507–525 nm. The molar absorption coefficients (ε) were observed in the range of 52,400–58,000 $dm^3\ mol^{-1}\ cm^{-1}$. The 4-methoxyphenyl derivatives **28**–**30** were slightly more bathochromic than **24**, there being the λ_{max} at 542 nm. The ε values of **28**–**30** were observed in the range of 55,400–71,200 $dm^3\ mol^{-1}\ cm^{-1}$. The fluorescence maxima (F_{max}) of **24**–**27** and **28**–**30** were observed in the range of 612–630 and 655–669 nm, respectively.

2.3. Density functional theory (DFT) calculations

The structure of indoline dye **24** was optimized by the B3LYP/3-21G* level [25]. Among considerable four isomers, the *Z*,*E*-isomer, there being methine moiety *Z*-form and double rhodanine *E*-form, was calculated to be most stable as shown in Fig. 3. The *E*-isomers in the double rodanine moiety were more stable than the *Z*-isomers. The *Z*-isomers in the methine moiety were more stable than the *E*-isomers

* Corresponding author. Tel.: +81(0)58 293 2601; fax: +81 (0)58 230 1893.
E-mail address: matsui@apchem.gifu-u.ac.jp (M. Matsui).

0143-7208/$ – see front matter © 2008 Elsevier Ltd. All rights reserved.
doi:10.1016/j.dyepig.2008.07.010

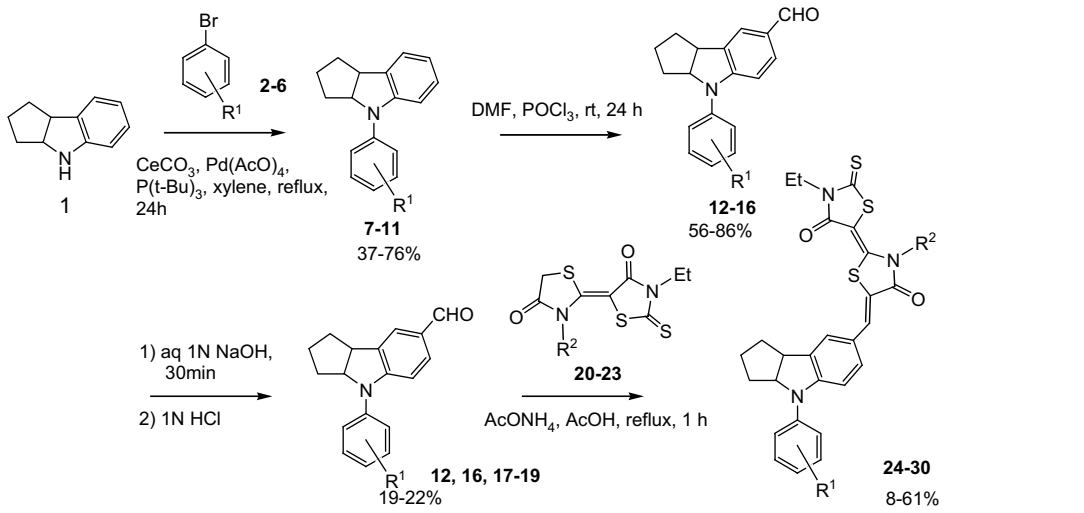

Compd	R^1
2, 7, 12	H
3, 8, 13	2-COOEt
4, 9, 14	3-COOEt
5, 10, 15	4-COOEt
6, 11, 16	4-OMe

Compd	R^1
17	2-COOH
18	3-COOH
19	4-COOH

Compd	R^2
20	CH_2COOH
21	Et
22	CH_2CH_2COOH
23	$CH_2CH_2CH_2COOH$

Compd	R^1	R^2
24	H	CH_2COOH
25	2-COOH	Et
26	3-COOH	Et
27	4-COOH	Et
28	4-OMe	CH_2COOH
29	4-OMe	CH_2CH_2COOH
30	4-OMe	$CH_2CH_2CH_2COOH$

Scheme 1.

due to steric hindrance between the hydrogen at the 6-position and carbony-oxygen in the inner rhodanine moiety. Consequently, the *Z,E*-isomer was most stable. The merocyanine chromophore is planar. The phenyl group on indoline moiety is twisted out of planar indoline moiety, the dihedral angle being 39.2°. The cyclopentane moiety is *syn*-form. The dihedral angle between the cyclopentane and planar indoline moieties is *ca.* 112°. Thus, the cyclopentane and phenyl moieties could act as bulky substituents for the planar merocyanine chromophore. The alkyl group on the terminal rhodanine ring might also act as a bulky substituent.

The first absorption band of indoline dyes was attributed to the HOMO–LUMO transition. The HOMO and LUMO electron densities of **24** are shown in Fig. 4. It is clear that first absorption band is an intramolecular charge-transfer chromophoric system from the indoline to rhodanine moiety.

2.4. Photoelectrochemical properties

The UV–vis absorption spectra of indoline dyes **24**–**27** and **28**–**30** on zinc oxide and their action spectra are shown in Figs. 5 and 6, respectively. The results are also summarized in Table 1. In all the cases, presence of cholic acid (CA) in dye-adsorption process improved the cell performance. For example, the η value of **28** in the presence of CA (4.53%, Table 1, run 5) was higher than that in the absence of CA 2.88% (incident photon-to-current efficiency (IPCE) 76%, short-circuit photocurrent density (J_{sc}) 10.24 A, open-circuit voltage (V_{oc}) 0.57 V, fill factor (ff) 0.49). Therefore, all the dye-adsorbed zinc oxide film was prepared in the presence of CA.

Slight difference in the UV–vis absorption spectra on zinc oxide was observed among **24**–**27** as depicted in Fig. 5a. This may be attributed to a different position of anchor group resulting in

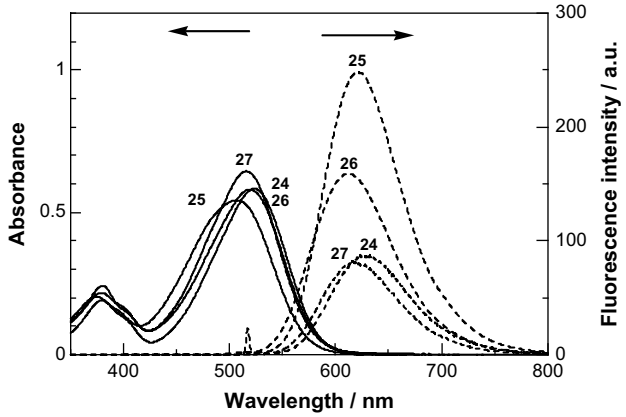

Fig. 1. UV–vis absorption and fluorescence spectra of **24**–**27**. Solid and dotted lines represent UV–vis absorption and fluorescence spectra, respectively. Measured at the concentration of 1×10^{-5} mol dm^{-3} in an acetonitrile/*tert*-butyl alcohol = 1:1 mixed solution at 25 °C.

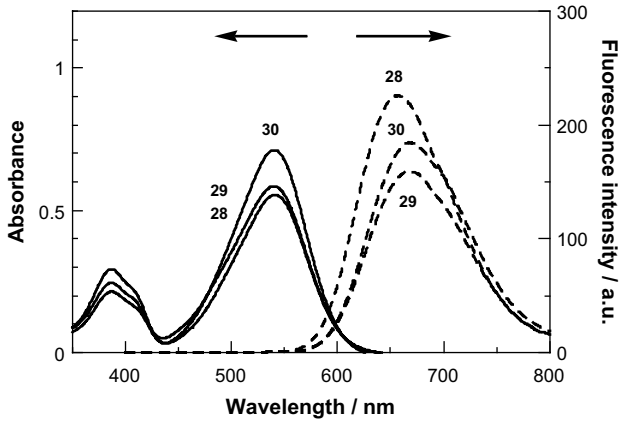

Fig. 2. UV–vis absorption and fluorescence spectra of **28**–**30**. Solid and dotted lines represent UV–vis absorption and fluorescence spectra, respectively. Measured at the concentration of 1×10^{-5} mol dm^{-3} in DMSO at 25 °C.

Table 1
Properties of indoline dyes

Run	Compound	λ_{max} (ε) (nm)	F_{max} (nm)	IPCE[c] (%)	J_{SC}[c] (mA cm^{-2})	V_{OC}[c] (V)	ff[c] (%)	η[c] (%)
1	**24**	525 (56,400)[a]	630[a]	87	10.63	0.63	0.64	4.31
2	**25**	507 (54,200)[a]	612[a]	51	5.12	0.62	0.61	1.92
3	**26**	519 (58,000)[a]	620[a]	27	4.78	0.59	0.57	1.60
4	**27**	515 (52,400)[a]	618[a]	41	5.00	0.63	0.67	2.10
5	**28**	542 (55,400)[b]	655[b]	81	12.11	0.62	0.61	4.53
6	**29**	541 (58,400)[b]	669[b]	68	9.55	0.56	0.64	3.43
7	**30**	542 (71,200)[b]	669[b]	66	9.44	0.63	0.62	3.69

[a] Measured in *tert*-butyl alcohol/acetonitrile = 1/1 (V/V) on $\times 10^{-5}$ mol dm^{-3} of substrate at 25 °C.
[b] Measured in DMSO on $\times 10^{-5}$ mol dm^{-3} of substrate at 25 °C.
[c] In all the cases, cholic acid (CA, 0.2 mM) was added during absorption process of dyes. Action spectra and I–V characteristics under AM 1.5 irradiation (100 mW cm^{-2}).

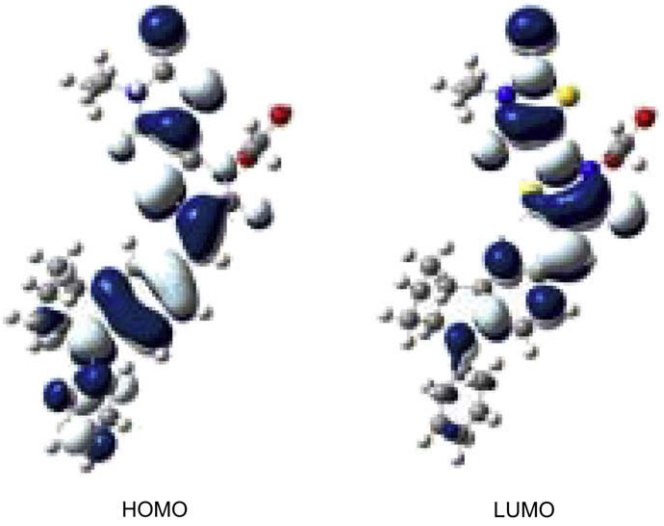

Fig. 4. HOMO and LUMO orbitals in **24**.

different interactions between the chromophore and zinc oxide. Fig. 5b indicates that indoline dye **24** shows the highest IPCE among **24**–**27**. As the shape of action spectra is similar, indoline dye **24** showed the largest J_{SC} value (10.63 mA cm^{-2}), resulting in the highest conversion efficiency (4.31%). The indoline dyes consist of intramolecular charge-transfer chromophoric system from the indoline to rhodanine moieties as shown in Fig. 4. Therefore, the introduction of anchor group into the electron-accepting rhodanine moiety could show better cell performance.

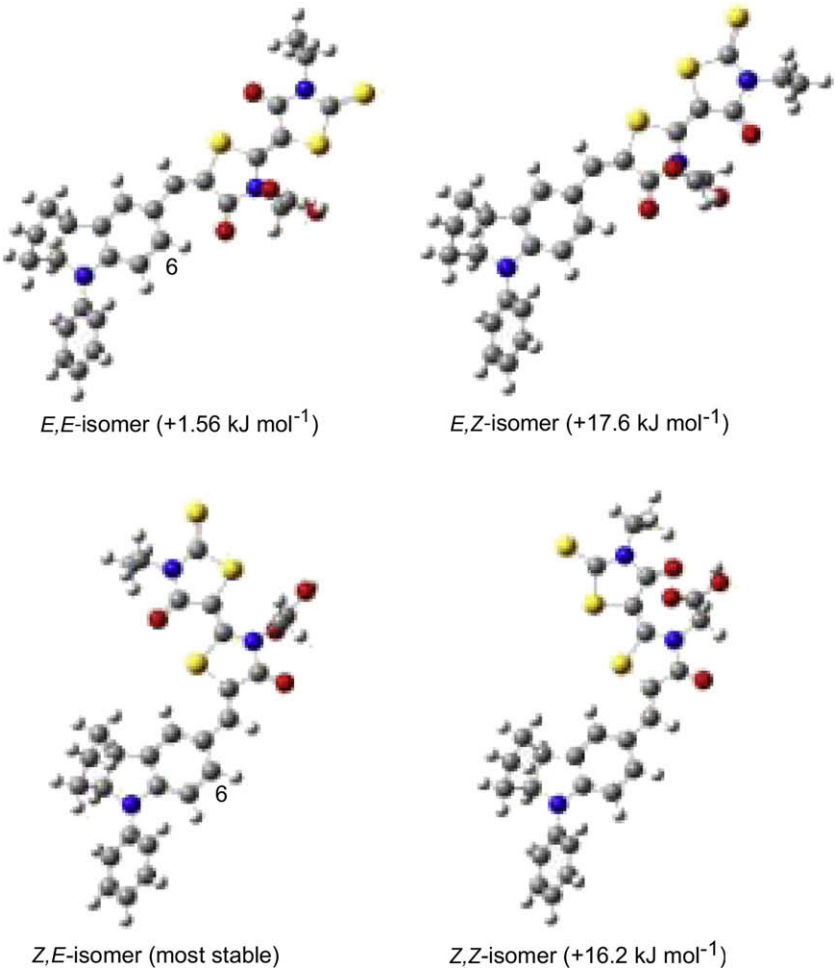

Fig. 3. Isomers for **24**.

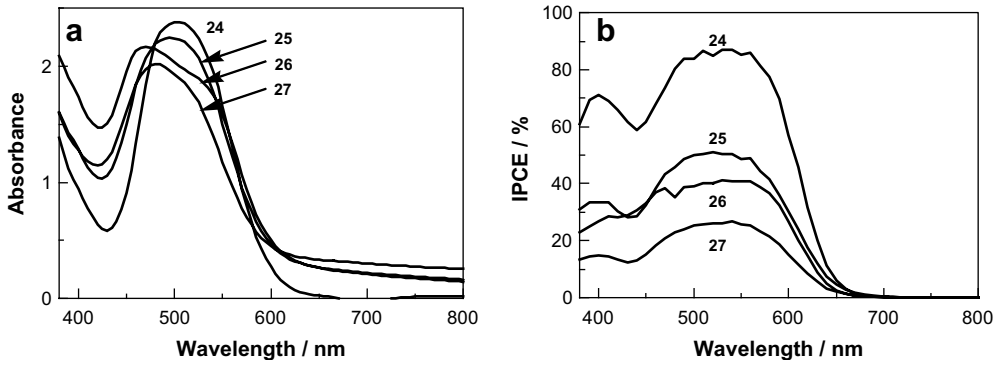

Fig. 5. (a) UV–vis absorption spectra of **24**–**27** and (b) action spectra of **24**–**27**.

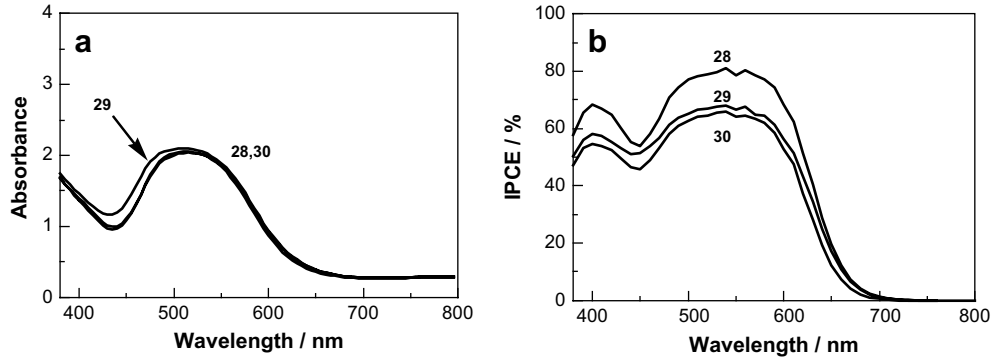

Fig. 6. (a) UV–vis absorption spectra of **28**–**30** on zinc oxide and (b) action spectra of **28**–**30**.

No remarkable difference in the UV–vis absorption spectra on zinc oxide was observed among **28**–**30** as shown in Fig. 6a. Fig. 6b indicates that **28** shows the highest IPCE among them. Thus, compound **28**, in which carboxymethyl group is attached to the rhodanine moiety, showed the highest conversion efficiency of 4.53% among **28**–**30**, due to the highest J_{sc} value (12.11 mA cm^{-2}). This result indicates that short contact between the indoline dye and zinc oxide is effective to accelerate electron injection to improve the cell performance. Consequently, the indoline dye **28** showed the highest η value among **24**–**30**, due to the highest J_{sc}.

3. Conclusion

The introduction of carboxymethyl group into the double rhodanine moiety was best to improve the performance of zinc oxide solar cell, due to the highest J_{sc}.

4. Experimental

4.1. Instruments

Melting points were measured with a Yanagimoto MP-52 micro-melting-point apparatus. NMR spectra were obtained by a Varian Inova 400 and 500 spectrometers. Mass spectra were taken on JEOL MStation 700 spectrometer. UV–vis absorption, fluorescence, and reflection spectra were taken on Hitachi U-3500, F-4500, and U-4000 spectrophotometers, respectively.

4.2. Materials

Compound **1** was supplied from Chemicrea Co. Ltd. Bromobenzene (**2**), ethyl 2-bromobenzoate (**3**), ethyl 3-bromobenzoate (**4**), ethyl 4-bromobenzoate (**5**), and 4-methoxybromobenzene (**6**) were purchased from Wako Co. Ltd. Double rhodanines **20**–**23** were prepared in a similar way as described in the literature [26].

4.3. Synthesis of *7*–*11*

To xylene (37 ml) were added 1,2,3,3*a*,4,8*b*-hexahydrocyclopenta[*b*]indole (**1**, 1.59 g, 10 mmol), aromatic bromides **2**–**6** (10 mmol), cesium carbonate (4.55 g, 14 mmol), palladium acetate (12 mg, 5.4×10^{-2} mmol), and tri-*tert*-butylphosphine (192 mg, 1 mmol). The mixture was refluxed for 24 h. After the reaction was completed, the mixture was filtered. The filtrate was washed with a saturated aqueous ammonium chloride (20 ml × 3). Compounds **7**, **9**, **10**, and **11** were purified by silica gel column chromatography (toluene). In the case of **8**, the washed mixture was used without further purification. The physical and spectral data are shown below.

4.3.1. *4-Phenyl-1,2,3,3*a*,4,8*b*-hexahydrocyclopenta[*b*]indole (**7**)*

Yield 74%; oil; ^{1}H NMR ($CDCl_3$) $\delta = 1.49$–1.59 (m, 1H), 1.61–1.70 (m, 1H), 1.80–1.96 (m, 3H), 2.00–2.09 (m, 1H), 3.82–3.86 (m, 1H), 4.73–4.78 (m, 1H), 6.73 (t, $J = 7.2$ Hz, 1H), 6.96 (t, $J = 6.9$ Hz, 1H), 7.02–7.05 (m, 2H), 7.12 (d, $J = 7.2$ Hz, 1H), 7.27–7.35 (m, 4H); EI-MS (70 eV) *m*/*z* (rel. intensity) 235 (M^+, 50), 206 (100).

4.3.2. *4-[2-(Ethoxycarbonyl)phenyl]-1,2,3,3*a*,4,8*b*-hexahydrocyclopenta[*b*]indole (**8**)*

Yield 37%.

4.3.3. *4-[3-(Ethoxycarbonyl)phenyl]-1,2,3,3*a*,4,8*b*-hexahydrocyclopenta[*b*]indole (**9**)*

Yield 50%; oil; ^{1}H NMR ($CDCl_3$) $\delta = 1.40$ (t, $J = 7.0$ Hz, 3H), 1.53–1.55 (m, 1H), 1.65–1.68 (m, 1H), 1.86–1.93 (m, 3H), 2.02–2.07 (m, 1H), 3.84–3.88 (m, 1H), 4.38 (q, $J = 7.0$ Hz, 2H), 4.77–4.81 (m, 1H),

6.77 (t, $J = 7.0$ Hz, 1H), 7.03–7.09 (m, 2H), 7.14 (d, $J = 7.0$ Hz, 1H), 7.39 (t, $J = 7.0$ Hz, 1H), 7.47 (d, $J = 7.0$ Hz, 1H), 7.61 (d, $J = 7.0$ Hz, 1H), 7.96 (s, 1H); EI-MS (70 eV) *m*/*z* (rel. intensity) 307 (M^+, 100), 278 (83).

*4.3.4. 4-[4-(Ethoxycarbonyl)phenyl]-1,2,3,3*a*,4,8*b*-hexahydrocyclopenta[*b*]indole (**10**)*

Yield 42%; oil; ^{1}H NMR ($CDCl_3$) $\delta = 1.39$ (t, $J = 6.8$ Hz, 3H), 1.46–1.51 (m, 1H), 1.64–1.69 (m, 1H), 1.89–1.96 (m, 3H), 2.05–2.08 (m, 1H), 3.87–3.90 (m, 1H), 4.35 (q, $J = 6.8$ Hz, 2H), 4.72–4.75 (m, 1H), 6.84 (t, $J = 8.0$ Hz, 1H), 7.11 (t, $J = 8.0$ Hz, 1H), 7.16 (d, $J = 8.0$ Hz, 1H), 7.20 (d, $J = 8.0$ Hz, 1H), 7.28 (d, $J = 7.8$ Hz, 2H), 7.99 (d, $J = 7.8$ Hz, 2H); EI-MS (70 eV) *m*/*z* (rel. intensity) 307 (M^+, 100), 278 (76).

*4.3.5. 4-(4-Methoxyphenyl)-1,2,3,3*a*,4,8*b*-hexahydrocyclopenta[*b*]indole (**11**)*

Yield 76%; oil; ^{1}H NMR ($CDCl_3$) $\delta = 1.51$–2.05 (m, 6H), 3.79–3.83 (m, 1H), 3.81 (s, 3H), 4.68–4.72 (m, 1H), 6.65 (t, $J = 7.8$ Hz, 1H), 6.71 (d, $J = 7.8$ Hz, 1H), 6.90 (d, $J = 8.4$ Hz, 2H), 6.99 (t, $J = 7.8$ Hz, 1H), 7.09 (d, $J = 7.8$ Hz, 1H), 7.21 (d, $J = 8.4$ Hz, 2H); EI-MS (70 eV) *m*/*z* (rel. intensity) 265 (M^+, 84), 278 (100).

*4.4. Synthesis of **12**–**16***

To DMF (15 ml) was added phosphoryl chloride (920 mg, 5.9 mmol). Then, to this mixture was added a DMF solution of **7**–**11** (5 mmol). The mixture was stirred for 1 day at room temperature. After the reaction was completed, to the mixture were added water (50 ml) and 1 N aqueous sodium hydroxide (100 ml) to adjust the pH value of the mixture higher than 10. The product was extracted with dichloromethane (150 ml × 3). After the extract was dried over anhydrous sodium sulfate, the solvent was removed *in vacuo*. The product was purified by silica gel column chromatography (dichloromethane) to give yellow oil. In the case of **13**, the crude product was used without further purification.

*4.4.1. 4-Phenyl-1,2,3,3*a*,4,8*b*-hexahydrocyclopenta[*b*]indole-7-carbaldehyde (**12**)*

Yield 70%; m.p. 120–122 °C; ^{1}H NMR ($CDCl_3$) $\delta = 1.49$–1.55 (m, 1H), 1.65–1.78 (m, 2H), 1.86–1.91 (m, 2H), 2.04–2.08 (m, 1H), 3.81–3.86 (m, 1H), 4.91–4.94 (m, 1H), 6.82 (d, $J = 8.3$ Hz, 1H), 7.13 (t, $J = 8.5$ Hz, 1H), 7.28–7.31 (m, 2H), 7.37–7.39 (m, 2H), 7.51 (d, $J = 8.3$ Hz, 1H), 7.63 (s, 1H), 9.70 (s, 1H); EI-MS (70 eV) *m*/*z* (rel. intensity) 263 (M^+, 57), 234 (100).

*4.4.2. 4-[2-(Ethoxycarbonyl)phenyl]-1,2,3,3*a*,4,8*b*-hexahydrocyclopenta[*b*]indole-7-carbaldehyde (**13**)*

Yield 70%.

*4.4.3. 4-[3-(Ethoxycarbonyl)phenyl]-1,2,3,3*a*,4,8*b*-hexahydrocyclopenta[*b*]indole-7-carbaldehyde (**14**)*

Yield 69%; oil; ^{1}H NMR ($CDCl_3$) $\delta = 1.41$ (t, $J = 7.2$ Hz, 3H), 1.50–1.56 (m, 1H), 1.63–1.73 (m, 1H), 1.85–1.93 (m, 3H), 2.07–2.11 (m, 1H), 3.86–3.89 (m, 1H), 4.40 (q, $J = 7.2$ Hz, 2H), 4.97–5.00 (m, 1H), 6.88 (d, $J = 8.3$ Hz, 1H), 7.45–7.51 (m, 2H), 7.55 (d, $J = 8.3$ Hz, 1H), 7.66 (s, 1H), 7.79 (d, $J = 7.3$ Hz, 1H), 7.98 (s, 1H), 9.73 (s, 1H); EI-MS (70 eV) *m*/*z* (rel. intensity) 335 (M^+, 100), 306 (74).

*4.4.4. 4-[4-(Ethoxycarbonyl)phenyl]-1,2,3,3*a*,4,8*b*-hexahydrocyclopenta[*b*]indole-7-carbaldehyde (**15**)*

Yield 56%; oil; ^{1}H NMR ($CDCl_3$) $\delta = 1.40$ (t, $J = 7.1$ Hz, 3H), 1.69–1.72 (m, 1H), 1.89–1.95 (m, 3H), 2.06–2.11 (m, 2H), 3.86–3.91 (m, 1H), 4.38 (q, $J = 7.1$ Hz, 2H), 4.93–4.97 (m, 1H), 7.11 (d, $J = 8.6$ Hz, 1H), 7.35 (d, $J = 8.8$ Hz, 2H), 7.60 (d, $J = 8.6$ Hz, 1H), 7.68 (s, 1H), 8.06 (d, $J = 8.8$ Hz, 2H), 9.77 (s, 1H); EI-MS (70 eV) *m*/*z* (rel. intensity) 335 (M^+, 85), 306 (100).

*4.4.5. 4-(4-Methoxyphenyl)-1,2,3,3*a*,4,8*b*-hexahydrocyclopenta[*b*]indole-7-carboaldehyde (**16**)*

Yield 86%; oil; ^{1}H NMR ($CDCl_3$) $\delta = 1.52$–1.54 (m, 2H), 1.67–1.70 (m, 2H), 1.86–1.88 (m, 2H), 2.03–2.07 (m, 1H), 3.84 (s, 3H), 4.83–4.86 (m, 1H), 6.55 (d, $J = 8.3$ Hz, 1H), 6.95 (d, $J = 8.8$ Hz, 2H), 7.21 (d, $J = 8.8$ Hz, 2H), 7.48 (d, $J = 8.3$ Hz, 1H), 7.61 (s, 1H), 9.67 (s, 1H); EI-MS (70 eV) *m*/*z* (rel. intensity) 293 (M^+, 100), 264 (94).

*4.5. Synthesis of 4-(carboxyphenyl)-1,2,3,3*a*,4,8*b*-hexahydrocyclopenta[*b*]indole-7-carbaldehyde **17**–**19***

To an ethanol solution (6 ml) of **13**–**15** (335 mg, 1 mmol) was added 1 N aqueous sodium hydroxide (0.2 ml). The mixture was refluxed for 30 min. After cooling, to the mixture were added water (10 ml) and 1 N hydrochloric acid (2 ml) to adjust the pH value to about 1. The product was extracted with dichloromethane (20 ml × 3) and purified by silica gel column chromatography (dichloromethane/methanol = 1/1). In the case of **17**, the crude product was used without further purification.

*4.5.1. 4-(2-Carboxyphenyl)-1,2,3,3*a*,4,8*b*-hexahydrocyclopenta[*b*]indole-7-carbaldehyde (**17**)*

Yield 22%.

*4.5.2. 4-(3-Carboxyphenyl)-1,2,3,3*a*,4,8*b*-hexahydrocyclopenta[*b*]indole-7-carbaldehyde (**18**)*

Yield 19%; m.p. >300 °C; ^{1}H NMR ($CDCl_3$) $\delta = 1.48$–1.92 (m, 6H), 3.87–3.91 (m, 1H), 4.97–5.00 (m, 1H), 6.93 (d, $J = 7.8$ Hz, 1H), 7.51 (t, $J = 8.4$ Hz, 1H), 7.56–7.58 (m, 2H), 7.68 (s, 1H), 7.85 (d, $J = 7.8$ Hz 1H), 8.05 (s, 1H), 9.79 (s, 1H); EI-MS (70 eV) *m*/*z* (rel. intensity) 307 (M^+, 77), 278 (100).

*4.5.3. 4-(4-Carboxyphenyl)-1,2,3,3*a*,4,8*b*-hexahydrocyclopenta[*b*]indole-7-carbaldehyde (**19**)*

Yield 19%; m.p. >300 °C; ^{1}H NMR ($CDCl_3$) $\delta = 1.19$–2.16 (m, 6H), 3.89–3.92 (m, 1H), 4.93–4.97 (m, 1H), 7.18 (d, $J = 8.4$ Hz, 1H), 7.39 (d, $J = 8.8$ Hz, 2H), 7.63 (d, $J = 8.4$ Hz, 1H), 7.71 (s, 1H), 8.13 (d, $J = 8.8$ Hz, 2H), 9.79 (s, 1H); EI-MS (70 eV) *m*/*z* (rel. intensity) 307 (M^+, 73), 278 (100).

*4.6. Synthesis of dyes **24**–**30***

To acetic acid (20 ml) were added **12**, **16**–**19** (1.0 mmol), double rhodanines **20**–**23** (1.0 mmol), and ammonium acetate (1 mg). The mixture was refluxed for 1 h. After the reaction was completed, to the mixture was added water. The resulting precipitate was filtered and purified by silica gel column chromatography (**24**–**27**: chloroform/methanol = 10/1, **28**–**30**: chloroform/methanol = 5/1). The physical and spectral data are shown below.

*4.6.1. Dye **24***

Yield 61%; m.p. 272–274 °C; ^{1}H NMR (DMSO-d_6) $\delta = 1.18$ (t, $J = 6.9$ Hz, 3H), 1.36–1.43 (m, 1H), 1.64–1.83 (m, 5H), 3.91–3.95 (m, 1H), 4.06 (q, $J = 6.9$ Hz, 2H), 4.78 (s, 2H), 5.06–5.09 (m, 1H), 7.00 (d, $J = 8.2$ Hz, 1H), 7.14 (t, $J = 6.9$ Hz, 1H), 7.37–7.49 (m, 6H), 7.75 (s, 1H); FAB-MS (NBA) *m*/*z* 564 (MH^+).

*4.6.2. Dye **25***

Yield 14%; m.p. >300 °C; ^{1}H NMR (DMSO-d_6) $\delta = 1.19$ (t, $J = 7.0$ Hz, 3H), 1.27 (t, $J = 7.0$ Hz, 3H), 1.62–2.09 (m, 6H), 4.02 (q, $J = 7.0$ Hz, 2H), 4.04–4.09 (m, 1H), 4.07 (q, $J = 7.0$ Hz, 2H), 5.03–5.08 (m, 1H), 6.23 (d, $J = 8.4$ Hz, 1H), 7.31 (d, $J = 8.4$ Hz, 1H), 7.38–7.43 (m, 2H), 7.51 (t, $J = 7.7$ Hz, 1H), 7.67 (t, $J = 7.7$ Hz, 1H), 7.67 (s, 1H), 7.86 (d, $J = 7.7$ Hz, 1H); FAB-MS (NBA) *m*/*z* 578 (MH^+).

*4.6.3. Dye **26***

Yield 8%; m.p. >300 °C; ^{1}H NMR (DMSO-d_6) $\delta = 1.19$ (t, $J = 7.0$ Hz, 3H), 1.27 (t, $J = 7.0$ Hz, 3H), 1.34–2.12 (m, 6H), 3.93–4.07 (m, 1H), 4.00 (q, $J = 7.0$ Hz, 2H), 4.07 (q, $J = 7.0$ Hz, 2H), 5.05–5.07 (m, 1H), 7.05 (d, $J = 9.2$ Hz, 1H), 7.38–7.47 (m, 2H), 7.55 (t, $J = 8.1$ Hz, 1H), 7.62–7.70 (m, 3H), 7.90 (s, 1H); FAB-MS (NBA) m/z 578 (MH^+).

*4.6.4. Dye **27***

Yield 19%; m.p. >300 °C; ^{1}H NMR (DMSO-d_6) $\delta = 1.19$ (t, $J = 7.1$ Hz, 3H), 1.28 (t, $J = 7.1$ Hz, 3H), 1.34–2.13 (m, 6H), 3.96–4.00 (m, 1H), 4.01 (q, $J = 7.1$ Hz, 2H), 4.07 (q, $J = 7.1$ Hz, 2H), 5.02–5.06 (m, 1H), 7.31 (d, $J = 9.2$ Hz, 1H), 7.46 (d, $J = 8.4$ Hz, 2H), 7.44–7.50 (m, 2H), 7.73 (s, 1H), 7.95 (d, $J = 8.4$ Hz, 2H); FAB-MS (NBA) m/z 578 (MH^+).

*4.6.5. Dye **28***

Yield 31%; m.p. >300 °C; ^{1}H NMR (DMSO-d_6) $\delta = 1.19$ (t, $J = 7.1$ Hz, 3H), 1.24–1.80 (m, 6H), 3.78 (s, 3H), 3.39–3.93 (m, 1H), 4.06 (q, $J = 7.1$ Hz, 2H), 4.71 (s, 2H), 4.98–5.03 (m, 1H), 6.71 (d, $J = 8.4$ Hz, 1H), 7.01 (d, $J = 8.6$ Hz, 2H), 7.33 (d, $J = 8.6$ Hz, 2H), 7.41 (d, $J = 8.4$ Hz, 1H), 7.43 (s, 1H), 7.72 (s, 1H); FAB-MS (NBA) m/z 594 (MH^+).

*4.6.6. Dye **29***

Yield 19%; m.p. >300 °C; ^{1}H NMR (DMSO-d_6) $\delta = 1.19$ (t, $J = 7.2$ Hz, 3H), 1.67–2.11 (m, 6H), 2.64 (t, $J = 8.1$ Hz, 2H), 3.78 (s, 3H), 3.88–3.92 (m, 1H), 4.07 (q, $J = 7.2$ Hz, 2H), 4.16 (t, $J = 8.1$ Hz, 2H), 4.98–5.00 (m, 1H), 6.70 (d, $J = 8.8$ Hz, 1H), 7.10 (d, $J = 8.4$ Hz, 2H), 7.32 (d, $J = 8.4$ Hz, 2H), 7.38 (d, $J = 8.8$ Hz, 1H), 7.40 (s, 1H), 7.67 (s, 1H); FAB-MS (NBA) m/z 608 (MH^+).

*4.6.7. Dye **30***

Yield 22%; m.p. >300 °C; ^{1}H NMR (DMSO-d_6) $\delta = 1.19$ (t, $J = 7.2$ Hz, 3H), 1.41–1.79 (m, 6H), 1.90 (quin, $J = 7.6$ Hz, 2H), 2.34 (t, $J = 7.6$ Hz, 2H), 3.78 (s, 3H), 3.88–3.96 (m, 1H), 4.02 (t, $J = 7.6$ Hz, 2H), 4.07 (q, $J = 7.2$ Hz, 2H), 4.98–5.04 (m, 1H), 6.71 (d, $J = 8.6$ Hz, 1H), 7.01 (d, $J = 9.0$ Hz, 2H), 7.32 (d, $J = 9.0$ Hz, 2H), 7.38 (d, $J = 8.6$ Hz, 1H), 7.41 (s, 1H), 7.67 (s, 1H); FAB-MS (NBA) m/z 622 (MH^+).

4.7. Film preparation and photoelectrochemical measurements

Zinc oxide film (thickness 3.0 μm) was prepared as described in the previous paper [20]. After desorption of Eosin Y, the film was dried at 150 °C for 1 h. The film was immersed in an acetonitrile/*tert*-butyl alcohol 1:1 mixed solution of dye (0.5 mmol dm^{-3}) containing cholic acid (1.0 mmol dm^{-3}) at room temperature. Then, the film was washed with an acetonitrile/*tert*-butyl alcohol 1:1 mixed solution. Acetonitrile–ethylenecarbonate (v/v = 1:4) containing tetrabutylammonium iodide (0.5 mol dm^{-3}) and iodine (0.05 mol dm^{-3}) was used as an electrolyte.

Action spectrum was obtained under monochromatic light with a constant photon number (0.05×1016 photon cm^{-2} s^{-1}). I–V characteristics were measured under illumination with AM 1.5 simulated sunlight (100 mW cm^{-2}) by using a Bunko-Keiki CEP-2000 system.

Acknowledgement

This work was financially supported in part by Grants-in-Aid for Science Research (No. 19550185) from Japan Society for the Promotion of Science (JSPS) and Research for Promoting Technological Seeds.

References

[1] Dentani T, Nagasaka K, Funabiki K, Jin JY, Yoshida T, Minoura H, et al. Flexible zinc oxide solar cells sensitized by styryl dyes. Dyes Pigments 2008;77:59–69.
[2] Wang ZS, Li FY, Huang CH. Photocurrent enhancement of hemicyanine dyes containing RSO_3^- group through treating TiO_2 films with hydrochloric acid. J Phys Chem B 2001;105:9210–7.
[3] Wang ZS, Li FY, Huang CH, Wang L, Wei M, Jim LP, et al. Photoelectric conversion properties of nanocrystalline TiO_2 electrodes sensitized with hemicyanine derivatives. J Phys Chem 2000;104:9676–82.
[4] Wang ZS, Hara K, Dan-oh Y, Kasada C, Shinpo A, Suga S, et al. Photophysical and (photo)electrochemical properties of a coumarin dye. J Phys Chem B 2005;109:3907–14.
[5] Hara K, Sato T, Katoh R, Furube A, Ohga Y, Shinpo A, et al. Molecular design of coumarin dyes for efficient dye-sensitized solar cells. J Phys Chem B 2003;107:597–606.
[6] Hara K, Kurashige M, Dan-oh Y, Kasada C, Shinpo A, Suga S, et al. Design for new coumarin dyes having thiophene moieties for highly efficient organic-dye-sensitized solar cells. New J Chem 2003;27:783–5.
[7] Hara H, Sayama K, Ohga Y, Shinpo A, Suga S, Arakawa H. A coumarin-derivative dye sensitized nanocrystalline TiO_2 solar cell having a high solar-energy conversion efficiency up to 5.6%. Chem Commun 2001:569–70.
[8] Liang M, Xu W, Cai F, Chen P, Peng B, Chen J, et al. New triphenylamine-based organic dyes for efficient dye-sensitized solar cells. J Phys Chem 2007;111:4465–72.
[9] Choi H, Lee JK, Song KJ, Song K, Kang SO, Ko J. Synthesis of new julolidine dyes having bithiophene derivatives for solar cell. Tetrahedron 2007;63:1553–9.
[10] Koumura N, Wang ZS, Mori S, Miyashita M, Suzuki E, Hara K. Alkyl-functionalized organic dyes for efficient molecular photovoltaics. J Am Chem Soc 2006;128:14256–7.
[11] Hagberg DP, Edvinsson T, Marinado T, Boschloo G, Hagfeldt A, Sun L. A novel organic chromophore for dye-sensitized nanostructured solar cell. Chem Commun 2006:2245–7.
[12] Hara K, Sato T, Katoh R, Furube A, Yoshihara T, Murai M, et al. Novel conjugated organic dyes for efficient dye-sensitized solar cells. Adv Funct Mater 2005;15:246–52.
[13] Kitamura T, Ikeda M, Shigaki K, Inoue T, Anderson NA, Ai X, et al. Phenyl-conjugated oligoene sensitizers for TiO_2 solar cell. Chem Mater 2004;16:1806–12.
[14] Jung I, Lee JK, Song KH, Song K, Kang SO, Ko J. Synthesis and photovoltaic properties of efficient organic dyes containing the benzo[*b*]furan moiety for solar cells. J Org Chem 2007;72:3652–8.
[15] Kim D, Lee JK, Kang O, Ko J. Molecular engineering of organic dyes containing *N*-aryl carbazole moiety for solar cell. Tetrahedron 2007;63:1913–22.
[16] Ito S, Zakeeruddin SM, Humphry-Baker R, Liska P, Charvet R, Comte P, et al. High-efficiency organic-dye-sensitized solar cells controlled by nanocrystal-line-TiO_2 electrode thickness. Adv Mater 2006;18:1202–5.
[17] Schmidt-Mende L, Bach U, Humphry-Baker R, Horiuchi T, Miura H, Ito S, et al. Organic dye for highly efficient solid-state dye-sensitized solar cell. Adv Mater 2005;17:813–5.
[18] Horiuchi T, Miura H, Uchida S. Highly efficient metal-free organic dyes for dye-sensitized solar cell. J Photochem Photobiol A Chem 2004;164:29–32.
[19] Horiuchi T, Miura H, Sumioka K, Uchida S. High efficiency of dye-sensitized solar cells based on metal-free indoline dyes. J Am Chem Soc 2004;126:12218–9.
[20] Yoshida T, Iwaya M, Ando H, Oekermann T, Nonomura K, Schlettwein D, et al. Improved photoelectrochemical performance of electrodeposited ZnO/EosinY hybrid thin films by dye re-adsorption. Chem Commun 2004:400–1.
[21] Otsuka A, Funabiki K, Sugiyama N, Mase H, Yoshida T, Minoura H, et al. Design and synthesis of near-infrared-active heptamethine-cyanine dyes to supress aggregation in a dye-sensitized porous zinc oxide solar cell. Chem Lett 2008;37:176–7.
[22] Komatsu D, Zhang J, Yoshida T, Minoura H. Electrochemical growth of ZnO/eosin Y hybrid thin film. Trans Mater Res Jpn 2007;32:417–20.
[23] Otsuka A, Funabiki K, Sugiyama N, Yoshida T, Minoura H, Matsui M. Dye sensitization of ZnO by unsymmetrical squaraine dyes suppressing aggregation. Chem Lett 2006;35:666–7.
[24] Oekermann T, Yoshida T, Tada H, Minoura H. Color-sensitive photoconductivity of nanostructured ZnO/dye hybrid films prepared by one-step electrodeposition. Thin Solid Films 2006;511–512:354–7.
[25] Frisch MJ, Trucks GW, Schlegel HB, Scuseria GE, Robb MA, Cheeseman JR, et al. Gaussian 03. Revision C.02. Wallingford, CT: Gaussian Inc; 2004.
[26] David AJ. Method of synthesizing methine dye intermediates, US 5679795 A. Chem Abstr 1997;127:347593.